Article

Symmetry invariants and classes of quasiparticles in magnetically ordered systems having weak spin-orbit coupling

Jian Yang[1], Zheng-Xin Liu [2,3] ✉ & Chen Fang [1,4] ✉

Symmetry invariants of a group specify the classes of quasiparticles, namely the classes of projective irreducible co-representations in systems having that symmetry. More symmetry invariants exist in discrete point groups than the full rotation group O(3), leading to new quasiparticles restricted to lattices that do not have any counterpart in a vacuum. We focus on the fermionic quasiparticle excitations under "spin-space group" symmetries, applicable to materials where long-range magnetic order and itinerant electrons coexist. We provide a list of 218 classes of new quasiparticles that can only be realized in the spin-space groups. These quasiparticles have at least one of the following properties that are qualitatively distinct from those discovered in magnetic space group(MSG)s, and distinct from each other:(i) degree of degeneracy,(ii) dispersion as function of momentum, and(iii) rules of coupling to external probe fields. We rigorously prove this result as a theorem that directly relates these properties to the symmetry invariants, and then illustrate this theorem with a concrete example, by comparing three 12-fold fermions having different sets of symmetry invariants including one discovered in MSG. Our approach can be generalized to realize more quasiparticles whose little co-groups are beyond those considered in our work.

In high-energy physics, elementary particles are classified into bosons and fermions, characterized by their different statistics, $(-1)^{2s}$, determined by their spin quantum number s, where $s(s+1)\hbar^2 = \mathbf{S}^2$. A similar distinction exists in their behavior under the anti-unitary time-reversal operation T, specifically $\hat{T}^2 = (-1)^{2s}$, with $\hat{T} = e^{i\hat{S}_y\pi/\hbar}K$[1], where $\hat{S}_y$ is the y-component of the spin operator $\hat{\mathbf{S}}$, and K is the complex-conjugate operator. The hatted quantities are the representations of operators acting on the single-particle Hilbert space. Therefore, the quantity $\hat{T}^2$, referred to as a symmetry invariant in later discussions, distinguishes fermions from bosons: $\hat{T}^2 = +1$ holds for particles with integer spin (bosons), while $\hat{T}^2 = -1$ is valid for those with half-odd-integer spin (fermions). About 60 years ago, Eugene Wigner first noted that the time-reversal invariant $\eta_T \equiv \hat{T}^2$ of elementary particles, as an

independent quantity, should not necessarily be related to $(-1)^{2s}$. This principle led to the proposal of additional types of elementary particles. Unfortunately, all particles discovered in high-energy physics satisfy constraint $\hat{T}^2 = (-1)^{2s}$ [2] (see Fig. 1), and Wigner's idea did not attract much attention.

In condensed matter physics, massless elementary particles like Dirac[3] or Weyl[4] fermions can emerge as quasiparticle excitations in the low-energy limit. Notably, since spatial symmetries (such as lattice translations and rotations) are discretized, symmetry invariants like $\eta_T = \hat{T}^2 = \pm 1$ and $\eta_{x,y}^S = (-1)^{2s} = \pm 1$ can take independent values, leading to the realization of new classes of particles proposed by Wigner. For instance, massless quasiparticles with $\hat{T}^2 \neq \eta_{x,y}^S$ can arise in electronic energy bands of systems with anti-ferromagnetic order, where

[1]Beijing National Laboratory for Condensed Matter Physics and Institute of Physics, Chinese Academy of Sciences, Beijing, China. [2]School of Physics and Beijing Key Laboratory of Opto-electronic Functional Materials and Micro-nano Devices, Renmin University of China, Beijing, China. [3]Key Laboratory of Quantum State Construction and Manipulation (Ministry of Education), Renmin University of China, Beijing, China. [4]Kavli Institute for Theoretical Sciences, Chinese Academy of Sciences, Beijing, China. ✉e-mail: liuzxphys@ruc.edu.cn; cfang@iphy.ac.cn

the nonsymmorphic time-reversal operation is associated with a fractional translation. New types of quasiparticles, illustrated in Fig. 1, exist in condensed matter physics, featuring $\hat{T}^2 = -1$ for bosons and $\hat{T}^2 = +1$ for fermions, without counterparts in high-energy physics. These emergent quasiparticles in materials are explored using the representation theory of groups. The symmetry operations of a system form a group, and point-like quasiparticle excitations are described by their projective irreducible co-representations (irReps). Specifically, quasiparticles and their corresponding projective irReps can be grouped into several projective classes specified by a set of discrete values of the symmetry invariants[5–11]. For example, time-like elementary particles in the standard model belong to two different projective classes (labeled by the symmetry invariant $\eta_{x,y}^S = \eta_T = \pm 1$) of the little group $O(3) \times Z_2^T$ for massive particles. In solids, the symmetry of a particle is reduced from continuous rotation O(3) to 32 subgroups known as crystallographic point groups. Thus, there is interest in the projective classes of $P \times Z_2^T$, where P is one of the 32 crystallographic point groups and Z_2^T is the time-reversal group. To date, researchers have enumerated all quasiparticles protected by type-II[12–26] and type-IV[8,9,27–44] Shubnikov's magnetic space groups (MSGs)[45–51]. Two questions naturally arise: (i) does this list exhaust the projective representations for symmetries of the form $P \times Z_2^T$? (ii) If not, where can we find the remaining quasiparticles? For the second question, recent advances in spin-space groups (SSGs) provide a clue, as they offer a complete description of the symmetries of magnetic orders beyond MSGs. SSGs also describe the symmetry of itinerant electrons hopping

on the magnetic lattice, provided the spin-orbit coupling (SOC) of the electrons is much smaller than the Zeeman splitting caused by the local magnetic moment[52–55]. Under weak SOC, unusual electronic structures and spin splittings emerge[56–59]. An increasing number of experimental and theoretical studies on magnetic materials with weak SOC, including *altermagnetism* with SSGs as approximate symmetries[55,60–67], have been conducted. Candidate materials include Mn_5Si_3[68], RuO_2[58,69], $MnTe$[70], $MnTe_2$[71], and $CoNb_3S_6$[53,72]. A few examples of new quasiparticles with spin point group symmetry have been theoretically predicted[52–54,72–74]. In addition, there are works discussing the representation theory and new quasiparticles of fermion and magnon bands within the framework of SSGs[75–77]. However, a comprehensive classification of these quasiparticles has yet to be accomplished.

In this paper, our results fully address the above open questions, using symmetry invariants as the primary tool. Symmetry invariants, a set of variables formed by factor systems, generate the second group-cohomology group and can be used to classify and identify the various projective classes for the same symmetry group. The projective classes form an intermediate layer between the groups and their (co)representations (Reps for short) and are less familiar to physicists. In Fig. 2, we summarize the relations among the groups, the projective classes, and the Reps, and also illustrate the correspondence between the physical entities (on the left) and the mathematical quantities (on the right). Generally, a symmetry invariant takes the value of a certain root of 1, but in the present work, it is always ± 1 valued (see "Methods" section for more details). For any given point group P, there are m_P number of $\mathbb{Z}_2$-valued symmetry invariants, resulting in 2^{m_P} projective classes and, consequently, 2^{m_P} quasiparticle types. We identify all these invariants and find the rigorous limit of 680 projective classes, or quasiparticle types, for all $P \times Z_2^T$ groups. Using the complete set of invariants, we show that all known quasiparticles protected by MSGs fall into 386 projective classes. To demonstrate that symmetry invariants provide not only a mathematical classification but also a physical classification of quasiparticles, we prove a theorem that any two quasiparticles with different values for symmetry invariants must differ in at least one of the following aspects: degeneracy, dispersion, or linear couplings to external fields. We then search for the remaining 294 quasiparticles unrealizable in MSGs and find that 218 can be realized in SSGs. Two of these are illustrated in detail to show their uniqueness: a spin-1/2 fermion with 12-fold degeneracy, as shown in Fig. 3, and another spin-1/2 fermion with 4-fold degeneracy, connected with 13 nodal lines, as shown in Fig. 4. We then attempt to scan magnetic materials with known magnetic structures for candidates hosting any of the 218 quasiparticles, and the search yields one candidate, Ce_3NIn.
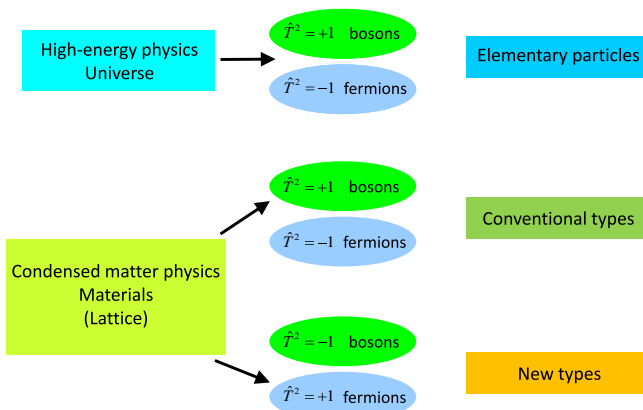

Fig. 1 | Types of (quasi)particles in high-energy physics and condensed matter physics. $\hat{T}^2 = +1$ for bosons and $\hat{T}^2 = -1$ for fermions are allowed in high-energy physics and condensed matter physics. But the new types, $\hat{T}^2 = -1$ for bosons and $\hat{T}^2 = +1$ for fermions, are only allowed in condensed matter physics.
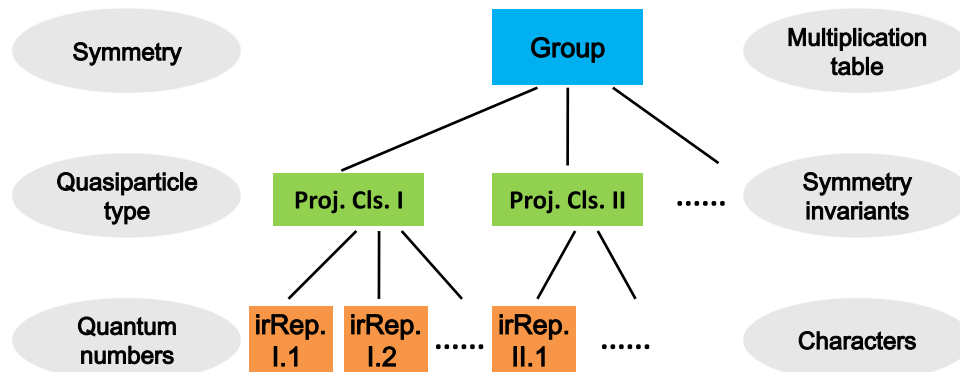

Fig. 2 | Group, projective class, and irRep. The projective classes are intermediate between the group and the irRep, with their corresponding physical concepts to the left, and the quantities that specify them on the right.
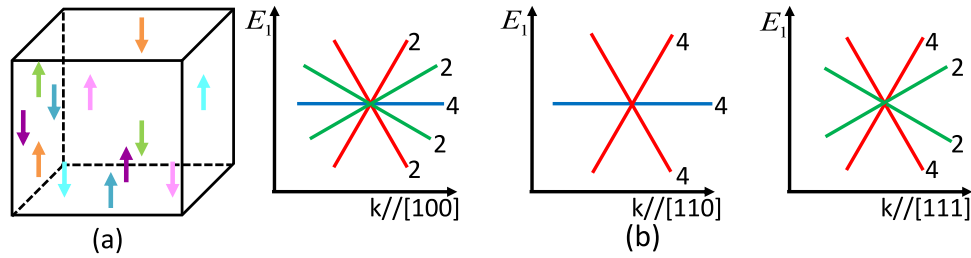
Fig. 3 | 12-fold fermions in spin-space group 229.2.1.9[87]. a A magnetic structure that is compatible with this SSG with 12 spins in one unit cell. The 12 spins are colored in orange, green, blue, purple, pink, and sky blue, each of which has upward and downward magnetic moments. **b** The schematic dispersion of the 12-fold fermion along three high-symmetry lines [100], [110], [111]. Along [100], the 12-fold fermion splits into one 4-fold band colored in blue, two 2-fold bands colored in red, and two 2-fold bands colored in green. Along [110], the 12-fold fermion splits into one 4-fold band colored in blue and two 4-fold bands colored in red. Along [111], the 12-fold fermion splits into two 4-fold bands colored in red and two 2-fold bands colored in green.
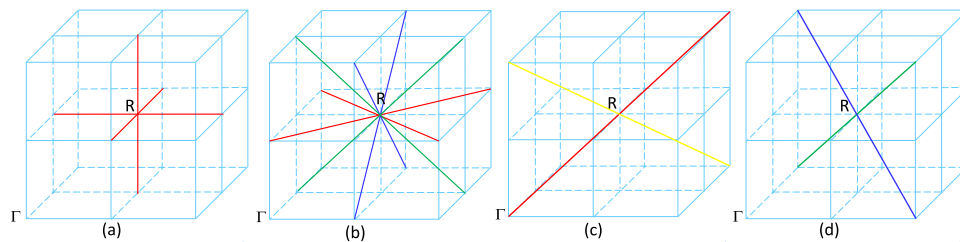

Fig. 4 | 13-nodal-line nexus in spin-space group 229.2.1.9[87]. The nodal lines meet at R in the magnetic BZ for the 13-nodal-line nexus. The nodal line degeneracies are exact because the irRep of R remains irreducible along the nodal lines. **a** The three red lines are nodal lines along k_x, k_y, and k_z directions. **b** The two red lines are nodal lines along $k_x \pm k_y$ directions, the two green lines are nodal lines along $k_x \pm k_z$ directions, and the two blue lines are nodal lines along $k_y \pm k_z$ directions. **c** The red line is a nodal line along $k_x + k_y + k_z$ direction, and the yellow line is a nodal line along $k_x + k_y - k_z$ direction. **d** The green line is a nodal line along $k_x - k_y + k_z$ direction, and the blue line is a nodal line along $k_x - k_y - k_z$ direction.

Results

Symmetry invariants of quasiparticles

We focus on quasiparticles with crystal momenta near a high-symmetry point in the Brillouin zone (BZ). Due to their high symmetry, these momenta are usually the centers of carrier pockets, around which effective models are constructed. In the long-wavelength limit, the quasiparticles move around a high-symmetry momentum and are thus subject to the little co-group at that momentum.

Assume the full symmetry of a Hamiltonian on a 3-dimensional lattice to be $\mathcal{G}$. The three lattice vectors define a translation group $\mathcal{T}$, which is a normal subgroup of $\mathcal{G}$. At $\mathbf{K} \in$ BZ, the little group $\mathcal{G}_\mathbf{K}$ is the subgroup of $\mathcal{G}$ that preserves $\mathbf{K}$ up to a reciprocal lattice vector, and we define the little co-group $G_\mathbf{K} \equiv \mathcal{G}_\mathbf{K}/\mathcal{T}$. With the translation symmetry "modded out", $G_\mathbf{K}$ describes the effective symmetries for quasiparticles at $\mathbf{K}$. Physically, a quasiparticle at $\mathbf{K}$ in this magnetic state is covariant under $G_\mathbf{K}$, and all observables are $G_\mathbf{K}$ symmetric.

The tricky part comes when the single-particle wavefunction, not observable by itself, is considered. The Bloch wavefunction transforms as a projective Rep $\rho(g)$, $g \in G_\mathbf{K}$[45,47,78,79], such that

$$\rho(g_1)\rho(g_2) = \omega_2(g_1, g_2)\rho(g_1 g_2), \qquad (1)$$

for g_1, g_2 being unitary. Throughout the paper, we use hatted operators $\hat{g}$ for the Rep of $g \in \mathcal{G}$ in the entire one-particle Hilbert space, and $\rho(g)$ for the Rep of $g \in G_\mathbf{K}$ in the subspace spanned by Bloch wavefunctions at $\mathbf{K}$. Compared with a Rep where $\rho(g_1)\rho(g_2) = \rho(g_1 g_2)$, Eq. (1) has a factor system $\omega_2(g_1, g_2) \in U(1)$. It is this factor system that gives rise to all types of the "new fermions"[8,17,32] and more quasiparticles to be discussed later. For crystallographic point groups, symmetry invariants are $\mathbb{Z}_2$-numbers that classify all factor systems for a given symmetry. For anti-unitary symmetries, the definition of projective

Rep slightly differs, and so does the form of symmetry invariants [See "Methods" section].

The most well-known example of projective Reps in physics is the half-odd-integer spin. The point group of a Galilean vacuum is $O(3) \times Z_2^T$, and if one takes two twofold axes 2_x and 2_y, then

$$\hat{2}_x \hat{2}_y = (-1)^{2s} \hat{2}_y \hat{2}_x. \qquad (2)$$

The symmetry invariant $\eta^S_{x,y} = (-1)^{2s} = -1$ represents the anti-commuting relation of $\hat{2}_x$ and $\hat{2}_y$ for all particles of half-odd-integer spins, like electrons, where the superscript S stands for the spin contribution. The time-reversal symmetry T introduces an additional invariant $\eta^S_T = \hat{T}^2 = -1$, which leads to the well-known Kramers degeneracy.

For a less known but important, example, we look at $\mathcal{G}$ being $P2_12_12_1 \times Z_2^T$ with three twofold screw axes $C_{2x} = \{2_x | \frac{1}{2}\frac{1}{2}0\}$, $C_{2y} = \{2_y | 0\frac{1}{2}\frac{1}{2}\}$, $C_{2z} = \{2_z | \frac{1}{2}0\frac{1}{2}\}$. One easily checks that $\hat{C}_{2i}\hat{C}_{2j} = \hat{t}_{x+y+z}\hat{C}_{2j}\hat{C}_{2i}$, for $i, j = x, y, z$, $i \neq j$ and $t_{x+y+z} \equiv \{E|111\}$. Now we look at phonons (bosons) near $\mathbf{K} = (\pi, \pi, \pi)$, where $G_\mathbf{K} = D_2 \times Z_2^T$. At $\mathbf{K}$, the translation operator $\hat{t}_{x+y+z}$ becomes -1, and we have

$$\rho(C_{2i})\rho(C_{2j}) = -\rho(C_{2j})\rho(C_{2i}) \qquad (3)$$

for $i \neq j$, yielding $\eta^L_{x,y} = -1$, where the superscript L stands for the lattice contribution. At the same time, T is simply time reversal and $\eta^L_T \equiv [\rho(T)K]^2 = +1$, with K being the complex conjugation. Comparing Eq. (2) and Eq. (3), one immediately finds that the phonons at $\mathbf{K}$ have $(\eta^L_{x,y} = -1, \eta^L_T = +1)$. On the other hand, for electrons at the same momentum point $\mathbf{K}$, the total invariants include the contribution from both the lattice and the spin and take the values $(\eta_{x,y} = \eta^L_{x,y}\eta^S_{x,y} = 1, \eta_T = \eta^L_T\eta^S_T = -1)$, with $\eta^S_{x,y} = -1$ and $\eta^S_T = -1$. This

combination of $(\eta_{x,y}, \eta_T)$ is what leads to the multi-chiral fermions known in transition-metal monosilicides[80–83]. From the two examples, we see that the symmetry invariants of $G_\mathbf{K}$ depend, and only depend, on (i) the fundamental spin, (ii) the symmetry group $\mathcal{G}$, and (iii) the crystal momentum $\mathbf{K}$, but not on any specifics of the band structure, such as the ordering of bands or the Fermi level. This property motivates one to classify quasiparticles using symmetry invariants. In the Supplementary Table I, the definitions of symmetry invariants in terms of the factor system are given, resulting in 680 quasiparticle types.

Where can we find materials that realize all these values for symmetry invariants? To be more precise, for a given point group P and specified values of invariants η, is there a lattice with symmetry $\mathcal{G}$ and a crystal momentum $\mathbf{K}$ such that $G_\mathbf{K} \cong P \times Z_2^T$ and the invariants correspond to those specified in η? For $\mathcal{G}$ being a type II MSG (that is, a space group (SG) times time reversal), 224 sets are realized; and for $\mathcal{G}$ being a type IV MSG (applicable to, e.g., antiferromagnets with doubled unit cells), an additional 162 sets are realized. In fact, for $P = C_{1,s,i,2,3,4,6,2v,3v,4v,6v,2h,3i}$, S_4, $D_{2,2d,2h}$, T, $T_{d,h}$, all sets of invariants can be realized in MSG. However, for $P = C_{3h,4h,6h}$, $D_{3,4,6,3d,3h,4h,6h}$, O, O_h, there are 294 sets of invariants that cannot be realized in MSG.

In MSG, spin-orbit coupling (SOC) requires every point-group operation $p \in O(3)$ to be associated with a spin rotation $\det[p]p \in SO(3)$. This means that the spin part of the operation is fixed by the spatial or lattice part of the operation. However, in the limit of negligible SOC, this locking between spin and space operations is released, which gives rise to more possibilities for the symmetry group. These new symmetries with unlocked spin and lattice operations, termed SSG[84,85], provide a way to realize more quasiparticles.

Structure of Spin-space groups

Now we investigate the structure of SSG, which provides important information for obtaining the invariants of quasiparticles. We consider the Hamiltonian for itinerant electrons in a magnetically ordered lattice

$$\hat{H} = \frac{\hat{\mathbf{p}}^2}{2m} + V(\mathbf{r}) + \mathbf{M}(\mathbf{r}) \cdot \hat{\mathbf{s}}, \tag{4}$$

where $\hat{\mathbf{s}}$ is the electron-spin operator, $V(\mathbf{r})$ the lattice potential, and $\mathbf{M}(\mathbf{r})$ the Zeeman/exchange field generated by the ordered moments. The spin symmetry rotations are not necessarily always locked with lattice rotations due to the absence of the SOC in Eq. (4)[52]. For example, in the magnetic material RuO_2[58,69] with collinear magnetic order along the x-axis, the C_{4z}^+ lattice rotation should be associated with C_{2z} spin rotation, characterized by an SSG symmetry $(C_{2z}||C_{4z}^+|\frac{1}{2}\frac{1}{2}\frac{1}{2})$. Such kinds of symmetry operations are called SSG operations, which form the spin-space groups. The absence of SOC in Eq. (4) unlocks the spatial and spin degrees of freedom of electrons from each other, enabling the realization of 218 new types of quasiparticles in SSG with little co-group $P \times Z_2^T$.

Generally, an SSG operation g has a spin part $\varphi_g \in SO(3) \times Z_2^T$ and a lattice part l_g, with $g = (\varphi_g || l_g)$. For later convenience, we define a unitarity indicator ζ_g such that $\zeta_g = 0$ if g is unitary and $\zeta_g = 1$ if g is anti-unitary. The lattice part can be represented as $l_g = \{p_g | \mathbf{t}_g\} T^{\zeta_g}$, which contains a point-group part $p_g \in O(3)$ and a translation vector $\mathbf{t}_g$. The spin rotation is decoupled from p_g, under the constraint that $\{(\varphi_g || l_g)\}$ forms a group under multiplication, which requires φ to be a homomorphism from the lattice part l_g to the spin part φ_g that preserves unitarity or anti-unitarity. A pseudo-vector field $\mathbf{M}(\mathbf{r})$ is said to be invariant under g if and only if $\mathbf{M}(\mathbf{r}) = s(\varphi_g)\mathbf{M}(l_g^{-1}\mathbf{r})$. Here, s is an "isomorphism" from $SO(3) \times Z_2^T$ to $O(3)$, i.e., a generalized vector Rep with $s(T) = -1_{3\times 3}$, $s(TR) = s(RT) = -s(R)$, and $s(R)$ being the usual vector Rep of R for $R \in SO(3)$.

Here we mention four key groups associated with the SSG $\mathcal{G}$[85]: (i) the group formed by the lattice part $\mathcal{L} = \{l_g | g \in \mathcal{G}\}$, (ii) the group formed by the spin part $S = \{\varphi_g | g \in \mathcal{G}\}$, (iii) all SSG operations that have a trivial spin part $\mathcal{L}_0 = \{l_g | g \in \mathcal{G}, \varphi_g = E\}$, and (iv) all SSG operations that have a trivial lattice part $S_0 = \{\varphi_g | g \in \mathcal{G}, l_g = \{E|\mathbf{0}\}\}$. From these definitions, it immediately follows that: (a) $\mathcal{L}$ is also the lattice part of an MSG $\mathcal{M}$ with $\mathcal{L} \cong \mathcal{M}$; (b) $\mathcal{L}_0$ is a normal subgroup of $\mathcal{L}$; (c) S is a subgroup of $SO(3) \times Z_2^T$, and S_0 is a normal subgroup of S. Symbolically, they are summarized in ref. 85 as:

$$\mathcal{L}_0 \triangleleft \mathcal{L}, S_0 \triangleleft S, \frac{\mathcal{L}}{\mathcal{L}_0} \cong \frac{S}{S_0} \cong \mathcal{G}/(\mathcal{L}_0 \times S_0). \tag{5}$$

Very recently, the SSGs have been completely enumerated with truncated sizes of magnetic unit cells[75,76,86–89]. In the present work, we mainly discuss cases where $S_0 = \{E\}$ is a trivial group. Under this assumption, $\mathcal{G} \cong \mathcal{M}$: an SSG with a trivial S_0 is isomorphic to an MSG. In the case of nontrivial S_0, our discussion also applies thanks to the relation $\mathcal{G}/S_0 \cong \mathcal{L} \cong \mathcal{M}$. We further restrict the discussion to cases where the magnetic unit cell is twice as large as the crystal unit cell, specifically considering SSGs that are: (i) isomorphic to type IV MSGs, and (ii) where nontrivial spin rotations are only associated with group elements that have nontrivial lattice point operations.

The difference between SSG $\mathcal{G}$ and the isomorphic MSG $\mathcal{M}$ then lies in the spin rotation φ_g for each $g \in \mathcal{L} \cong \mathcal{M}$, which is a homomorphism from $\mathcal{L}$ to $SO(3) \times Z_2^T$. First, we observe that $\mathcal{L}_0$ is the kernel of this homomorphism that maps to $1_{3\times 3}$. Then, we build a surjective homomorphism from $\mathcal{L}$ to the quotient group $\mathcal{L}/\mathcal{L}_0$ and then an injective homomorphism to $O(3)$:

$$\mathcal{L} \xrightarrow{\varphi} \frac{\mathcal{L}}{\mathcal{L}_0} \xrightarrow{s} O(3), g \mapsto \varphi_g \mapsto s(\varphi_g), \tag{6}$$

under the constraint $\det[s(\varphi_g)] = +1(-1)$ if g is unitary (anti-unitary). For each $\mathcal{L}$ and its normal subgroups $\mathcal{L}_0$, the quotient group $\mathcal{L}/\mathcal{L}_0$ is finite, thus there are a finite number of homomorphisms $s \cdot \varphi$. A similar structure also appears in the later discussion of the little co-group of quasiparticles.

Now we relate SSG to operators that act on electrons subject to $\mathbf{M}(\mathbf{r})$ as in Eq. (4). Under an SSG operation $g = (\varphi_g || l_g)$, an electron operator $c_\alpha(\mathbf{r})$, α, β being spin index, transforms as

$$c_\alpha^\dagger(\mathbf{r}) \xrightarrow{g} \sum_\beta d_{\beta\alpha}(\varphi_g) K^{\zeta_g} c_\beta^\dagger(l_g^{-1}\mathbf{r}), \tag{7}$$

where $d(\varphi_g)K^{\zeta_g} = u(s(\varphi_g))$ for unitary g and $d(\varphi_g)K^{\zeta_g} = u(s(T\varphi_g))(i\sigma_y K)$ for anti-unitary g, u: $SO(3) \to SU(2)$ is the natural embedding from $SO(3)$ to $SU(2)$.

Symmetry invariants of spin-space groups

An SSG $\mathcal{G}$ has a normal translation subgroup $\mathcal{T}_0 \triangleleft \mathcal{L}_0$. Using $\mathcal{T}_0$, the BZ and the crystal momentum $\mathbf{K}$ are defined. The little group $\mathcal{G}_\mathbf{K}$ is the subgroup of $\mathcal{G}$ preserving $\mathbf{K}$, and the little co-group $G_\mathbf{K} = \mathcal{G}_\mathbf{K}/\mathcal{T}_0$ is essentially a spin point group[90,91] whose elements are given by $(\varphi_p || p)$. The lattice parts p of $(\varphi_p || p)$ form $L_\mathbf{K}$, the little co-group of $\mathcal{L}$. As $\mathcal{G} \cong \mathcal{M} \cong \mathcal{L}$, we have $G_\mathbf{K} \cong M_\mathbf{K} \cong L_\mathbf{K}$ with $M_\mathbf{K}$, the little co-group of $\mathcal{M}$, recalling that the SSG $\mathcal{G}$ and the MSG $\mathcal{M}$ have the same pure translation part of $\mathcal{L}$.

The symmetry invariants may come from the spin part, as in Eq. (2), and the lattice part, as in Eq. (3). Each invariant of $G_\mathbf{K}$ hence factors into the lattice and the spin invariant $\eta_i = \eta_i^L \eta_i^S$. The lattice part of $G_\mathbf{K}$ is nothing but $M_\mathbf{K}$, the invariants of which can be computed as

$$\eta_{p_1,p_2}^L = \exp[-i(\mathbf{K}_{p_1} \cdot \mathbf{t}_{p_2} - \mathbf{K}_{p_2} \cdot \mathbf{t}_{p_1})] \tag{8}$$

if p_1, p_2 are unitary with $p_1 p_2 = p_2 p_1$ and

$$\eta_p^L = \exp(-i\mathbf{K}_p \cdot \mathbf{t}_p), \tag{9}$$

if p is anti-unitary with $p^2 = E$. Here the reciprocal lattice vector $\mathbf{K}_p$ is defined as $\mathbf{K}_p = (-1)^{\zeta_p}(p^{-1}\mathbf{K} - \mathbf{K})$ with $\zeta_p = 0(1)$ if p is unitary (anti-unitary)[47,92,93], $\mathbf{t}_p$ is the translation vector of p.

The spin part of $G_\mathbf{K}$, which is essentially a homomorphism from $L_\mathbf{K}$ to $SO(3) \times Z_2^T$ then to $O(3)$, can be classified and enumerated in the following way. First, $L_{0\mathbf{K}}$, the little co-group of $\mathcal{L}_0$ is the kernel of this mapping. For a given $L_\mathbf{K}$, there is a finite number of $L_{0\mathbf{K}}$, and for each given $L_{0\mathbf{K}}$, one can enumerate the mappings from the quotient group $L_\mathbf{K}/L_{0\mathbf{K}}$ to $O(3)$. Such a mapping $s \cdot \varphi: L_\mathbf{K} \to O(3)$ is a 3-dimensional real Rep of $L_\mathbf{K}$. With φ specified, the spin part of the invariants is

$$\eta_{p_1, p_2}^S \cdot 1_{2\times 2} = d(\varphi_{p_1})d(\varphi_{p_2})d^{-1}(\varphi_{p_1})d^{-1}(\varphi_{p_2}), \tag{10}$$

for unitary elements p_1, p_2 with $p_1 p_2 = p_2 p_1$ and

$$\eta_p^S \cdot 1_{2\times 2} = [d(\varphi_p)K]^2, \tag{11}$$

for anti-unitary element p with $p^2 = E$.

We focus on those SSGs, and the momentum points $\mathbf{K}$ which have $G_\mathbf{K} \cong P \times Z_2^T$. Remembering that $\mathcal{G} \cong \mathcal{M} \cong \mathcal{L}, G_\mathbf{K} \cong M_\mathbf{K} \cong L_\mathbf{K}$, and noticing that the MSG $\mathcal{M}$ and magnetic point group $M_\mathbf{K}$ can be easily identified from the standard crystallographic table, for convenience, we denote $M_\mathbf{K} = P \times Z_2^T$ (this, in turn implies that $\mathcal{M}$ is a type IV MSG). In Supplementary Table II, we have computed $P = C_{3h,4h,6h}$, $D_{3,4,6,3d,3h,4h,6h}$, O, O_h, the lattice-part invariants η^L. For the spin part, in Supplementary Tables III–XIV, we have listed the choice of $L_{0\mathbf{K}}$, the choice of homomorphism φ, and the resultant invariants η^S. For easy reference, each unique set of $\eta^{L/S}$ is labeled by a Boolean vector $(1 - \eta^{L/S})/2$, and the η^s leading to invariants only realizable in SSG are in RED. Finally, we obtain the full symmetry invariants for $G_\mathbf{K}$ using $\eta_i = \eta_i^L \eta_i^S$, listed in Supplementary Tables XV–XXVI. The η's that can be realized in type II and type IV MSG are colored in GREEN and BLUE, respectively, and those only realizable in SSG, counting 218, are in RED. The BLACK sets of invariants cannot be realized in MSG or even SSG. For each RED set, we have listed all possible pairs (η^L, η^S).

Physical properties determined by invariants

Now we show that, for a given $P \times Z_2^T$, two quasiparticles from different projective classes have distinct physical properties. They can differ from each other in the degrees of degeneracy. Otherwise, they are distinguished by the dispersion or the coupling to an external probe field, such as the displacement (phonon) field and the Zeeman field. First, we observe that any dispersion ϕ as a function of momentum, or any external field ϕ, corresponds to a linear irRep of $P \times Z_2^T$, so its components ϕ_i^μ carry a linear irRep of $P \times Z_2^T$, where $\mu(P \times Z_2^T)$ is a linear irRep and $i = 1, \cdots, \dim[\mu]$ labels the component within the irRep.

Then we notice that as the fermion operator $c_m^\dagger$ transforms as a projective irRep ρ with $m = 1, ..., \dim[\rho]$, the bilinear $c_m^\dagger c_n$ transforms as a linear Rep $\rho \otimes \rho^{*9}$, which reduces into direct sums of linear irRep μ: $\rho \otimes \rho^* = \sum_\mu \oplus N_\rho(\mu)\mu$, where the multiplicity[94]

$$N_\rho(\mu) = \frac{1}{2|P|}\sum_{g\in P}\left[|\chi^{(\rho)}(g)|^2\chi^{(\mu)}(g) + \omega_2(gT, gT)\chi^{(\rho)}\big((gT)^2\big)\chi^{(\mu)}(gT)\right] \tag{12}$$

is the number of times the linear irRep μ occurs in the direct product Rep $\rho \otimes \rho^*$. Here, $\chi^{(\rho)}(g)$ stands for the character of $g \in P$ in the projective irRep ρ, and $\chi^{(\mu)}(g)$ is the character of g in the linear irRep μ. $|P|$ is the number of elements in the point group P. The elements of the $\dim[\rho] \times \dim[\rho]$ matrix $\Gamma^{(\mu)\tau_\mu i}$ are the Clebsch-Gordon coefficients

combining the bases of the direct product Rep $\rho \otimes \rho^*$ into the i-th base of the linear irRep μ, where $\tau_\mu = 1, \ldots, N_\rho(\mu)$.

In terms of ϕ_i^μ and $\Gamma^{(\mu)\tau_\mu i}$, the general symmetric coupling takes the form

$$\hat{H} = \sum_{\mu, \tau_\mu, i} \lambda_{\tau_\mu}^{(\mu)}\phi_i^\mu\Gamma^{(\mu)\tau_\mu i}, \tag{13}$$

where coupling parameter $\lambda_{\tau_\mu}^{(\mu)} \in \mathbb{R}$. From Eq. (13), we see that the physical response of a quasiparticle (denoted by the corresponding irRep ρ) entirely depends on $N_\rho(\mu)$. For example, letting $P = O_h$ and identifying ϕ as momentum $\mathbf{k}$, which transforms as T_{1u}^- (− means odd under time reversal), if $N_\rho(T_{1u}^-) = 0$, then there is no linear dispersion for this quasiparticle. On the other hand, if $N_\rho(T_{1u}^-) = 2$, then there are two independent coupling parameters denoted as $\lambda_1^{(\mu)}$ and $\lambda_2^{(\mu)}$, hence two Fermi velocities for this quasiparticle. The same procedure applies if ϕ stands for probing Zeeman field (T_{1g}^- Rep), lattice displacement field (T_{1u}^+ Rep), strain tensor field (T_{2g}^+ Rep or E_g^+ Rep), and so on.

In Supplementary Note 3, we prove a theorem stating that if projective irReps ρ_1 and ρ_2 for $P \times Z_2^T$ belong to different projective classes (namely, ρ_1 and ρ_2 have different values of symmetry invariants), then there must exist at least one linear Rep μ such that $N_{\rho_1}(\mu) \neq N_{\rho_2}(\mu)$. Hence, when dispersion ϕ or external probe field ϕ carries a linear Rep μ, the quasiparticle carrying irRep ρ_1 must behave differently compared to the quasiparticle carrying irRep ρ_2. This seals the conclusion that any one of the 218 new quasiparticle types has distinct physical properties from the 386 types realizable in MSG, and the 218 classes of new quasiparticles also have distinct physical properties from each other. This is one of the central conclusions of the present work. In the next section, we will illustrate this result with concrete examples, namely, by comparing three 12-fold quasiparticles having different sets of symmetry invariants.

In Supplementary Tables XV–XXVI, we have summarized all band degeneracies for every set of symmetry invariants that are only realizable in SSG colored in RED, if the minimal dimension of (co)Reps is FOUR or higher, including the degree of degeneracy, the lowest-order dispersion, and the direction of the nodal lines (if any) meeting at this point.

Example: 12-fold fermions and 13 Dirac nodal lines

According to Supplementary Table XXVI, for $G_\mathbf{K} = O_h \times Z_2^T$, Invariants $\equiv (\eta_{C_{2x}, c_{2y}}, \eta_T, \eta_{IT}, \eta_{TC_{2a}}, \eta_{I,C_{2a}})$, when the five invariants take the values $\vec{\eta} = (+1, +1, -1, -1, -1)$, the corresponding projective class is only realizable in spin-space groups. One such example is the non-coplanar SSG 229.2.1.9 in the database[87], which is isomorphic to type IV MSG $\mathcal{M} = 223.109$. The elements of the SG $\mathcal{L}_0 \equiv Pm\bar{3}n(223)$ are pure lattice operations with a quotient group $229.2.1.9/223 \cong Z_2^T$. The little co-group at the high-symmetry point $R = (\pi, \pi, \pi)$ is $G_\mathbf{K} = O_h \times Z_2^T$, which is generated by $(E||C_{2x,2y,2z}, C_{2\mathbf{n}}, I)$ and $(T||TC_{2x,2y,2z}, TC_{2\mathbf{n}}, TI)$ as listed in Supplementary Table XIV, where I is spacial inversion, and $\mathbf{n}$ is a unit vector in the $\hat{x} \pm \hat{y}, \hat{x} \pm \hat{z}, \hat{y} \pm \hat{z}$ directions.

To obtain the magnetic configuration, we first illustrate a collinear configuration with 12 spins at the 12d Wyckoff positions in each unit cell, as shown in Fig. 3a. This configuration has a collinear SSG symmetry 229.2.1.3.L. The complete non-coplanar spin configuration actually contains three or more sets of collinear configurations (for instance, another two sets may be located at two inequivalent 24 g Wyckoff positions) with the condition that the directions of different sets of spins are mutually unparallel. Hence, the final configuration is a non-coplanar magnetic order described by the SSG 229.2.1.9. Similarly, the configuration of the coplanar SSG 229.2.1.6.P can be obtained if the number of collinear sets is two. The three groups, 229.2.1.3.L,

229.2.1.6.P, and 229.2.1.9, have the same lattice operations and only differ by their spin-only groups with $S_0 = SO(2) \rtimes Z_2^{C_{2x}T}, Z_2^{C_{2z}T}, \{E\}$ respectively. Furthermore, for the common little co-group symmetry $O_h \times Z_2^T$ at the R point, the three groups 229.2.1.3.L, 229.2.1.6.P, 229.2.1.9 have the same values of symmetry invariants, $(+1, +1, -1, -1, -1)$.

This set of invariants $\vec{\eta} = (+1, +1, -1, -1, -1)$ for $O_h \times Z_2^T$ allows a 12-dimensional irRep given by

$$\rho_1(C_{2i}) = \tau_0\sigma_0 e^{-iL_i\pi}, \quad \rho_1(C_{2\mathbf{n}}) = i\tau_z\sigma_0 e^{-i\mathbf{L}\cdot\mathbf{n}\pi},$$
$$\rho_1(I) = i\tau_x\sigma_0 1_{3\times3}, \qquad \rho_1(T)K = \tau_y\sigma_y 1_{3\times3}K, \tag{14}$$

whose dimensionality is higher than any known (co)Reps appearing in MSGs[9]. Here $L_{x,y,z}$ are the three components of angular momentum for $l = 1$, $\tau_0(\sigma_0) = 1_{2\times2}$, $\tau_{x,y,z}(\sigma_{x,y,z})$ are three Pauli matrices acting on the sublattice (spin) sector, $\mathbf{n}$ is a unit vector in $\hat{x}\pm\hat{y}, \hat{x}\pm\hat{z}, \hat{y}\pm\hat{z}$ directions. $\rho_1 \otimes \rho_1^*$ can be decomposed into linear irReps of $O_h \times Z_2^T$:

$$\rho_1 \otimes \rho_1^* = \cdots \oplus 4T_{1u}^- \oplus \cdots, \tag{15}$$

the linear irRep $\mu = T_{1u}^-$ corresponds to linear dispersion, the components $\phi_1^\mu = k_x, \phi_2^\mu = k_y, \phi_3^\mu = k_z$. Since multiplicity $N_{\rho_1}(T_{1u}^-) = 4$, there are 4 coupling parameters $\lambda_1^{(\mu)} = v_{1x}, \lambda_2^{(\mu)} = v_{1y}, \lambda_3^{(\mu)} = v_{1z}, \lambda_4^{(\mu)} = v_1'$. According to Eq. (13), the $\mathbf{k}\cdot\mathbf{p}$ model to the lowest order in $\mathbf{k}$, the crystal momentum relative to $\mathbf{K}$, takes the form

$$\hat{H}_1(\mathbf{k}) = (v_{1x}\tau_z\sigma_x + v_{1y}\tau_z\sigma_y + v_{1z}\tau_z\sigma_z)\mathbf{k}\cdot\mathbf{L} + v_1'\tau_y\sigma_0\mathbf{k}\cdot\mathbf{L}', \tag{16}$$

where $L_i' \equiv |\epsilon_{ijk}|\{L_j, L_k\}$, and $v_{1x,1y,1z}, v_1'$ material dependent Fermi velocity. This 12-fold degeneracy is a superposition of four spin-1 double-Weyl points, two with Chern number $+2$, and the other two -2. The linear dispersion and band splitting of this degeneracy along different high-symmetry lines are shown in Fig. 3b. Since there are no 12-dimensional irReps of $O_h \times Z_2^T$ in MSGs, the 12-fold fermion (14) is qualitatively different from all quasiparticles with symmetry group $O_h \times Z_2^T$ in MSGs because of the degree of degeneracy.

This 12-dimensional irRep appears at the R point of the three SSGs 229.2.1.3.L, 229.2.1.6.P, and 229.2.1.9, even though their S_0 are different (the difference in S_0 indeed has a consequence in their irReps. For instance, both 229.2.1.3.L and 229.2.1.6.P have an 8-dimensional irRep at the R point but the non-coplanar group 229.2.1.9 does not).

With the same invariants $\vec{\eta} = (+1, +1, -1, -1, -1)$, as shown in Supplementary Table XXVI, there is a 4-dimensional irRep[9]

$$\rho_0(C_{2i}) = \tau_0\sigma_0, \quad \rho_0(C_{2,01\bar{1}}) = i\tau_0\sigma_z,$$
$$\rho_0(C_{2,110}) = (i/2)\tau_0\sigma_z + (\sqrt{3}i/2)\tau_z\sigma_x,$$
$$\rho_0(I) = i\tau_z\sigma_y, \quad \rho_0(T)K = \tau_x\sigma_x K. \tag{17}$$

What is special about this fourfold degeneracy is that the band splitting around this point is proportional to k^5, unprecedented in previously studied symmetry-protected band nodes:

$$E(\mathbf{k}) = |k_x k_y k_z| \sqrt{3\left(k_x^2 - k_y^2\right)^2 + \left(2k_z^2 - k_x^2 - k_y^2\right)^2} + O(k^6). \tag{18}$$

Furthermore, as shown in Fig. 4, all high-symmetry directions around R are Dirac nodal lines, forming a 13-nodal-line-nexus where all lines remain fourfold degenerate. Since there are no 4-fold fermions with symmetry group $O_h \times Z_2^T$ having quintic band splitting dispersion in MSGs, our 4-fold fermion (17) with 13-nodal-line-nexus only realizable in SSGs is qualitatively different from 4-fold fermions with symmetry group $O_h \times Z_2^T$ realized in MSGs.

Aside from the 12-fold fermion (14), another 12-fold fermion can also only appear in SSGs with different values of invariants. For instance, at the R point, the SSG 229.2.2.36 has the invariants $(+1, -1, -1, +1, -1)$ for the little co-group $O_h \times Z_2^T$, which differ from the invariants of (14) only by η_T and $\eta_{TC_{2a}}$. The corresponding 12-dimensional irRep reads,

$$\rho_2(C_{2i}) = \tau_0\sigma_0 e^{-iL_i\pi}, \quad \rho_2(C_{2\mathbf{n}}) = i\tau_0\sigma_y e^{-i\mathbf{L}\cdot\mathbf{n}\pi},$$
$$\rho_2(I) = \tau_0\sigma_z 1_{3\times3}, \qquad \rho_2(T)K = i\tau_y\sigma_0 1_{3\times3}K. \tag{19}$$

$\rho_2 \otimes \rho_2^*$ can be decomposed into linear irReps of $O_h \times Z_2^T$:

$$\rho_2 \otimes \rho_2^* = \cdots \oplus 6T_{1u}^- \oplus \cdots. \tag{20}$$

The 12-fold fermion also has linear dispersion $\mu = T_{1u}^-$ with the components $\phi_1^\mu = k_x, \phi_2^\mu = k_y, \phi_3^\mu = k_z$. Since multiplicity $N_{\rho_2}(T_{1u}^-) = 6$, there are 6 coupling parameters $\lambda_1^{(\mu)} = v_{2x}, \lambda_2^{(\mu)} = v_{2y}, \lambda_3^{(\mu)} = v_{2z}, \lambda_4^{(\mu)} = v_{2x}', \lambda_5^{(\mu)} = v_{2y}', \lambda_6^{(\mu)} = v_{2z}'$. According to Eq. (13), the linear dispersion of the 12-fold fermion takes the form

$$\hat{H}_2(\mathbf{k}) = (v_{2x}\tau_x\sigma_y + v_{2y}\tau_y\sigma_y + v_{2z}\tau_z\sigma_y)\mathbf{k}\cdot\mathbf{L}$$
$$+ (v_{2x}'\tau_x\sigma_x + v_{2y}'\tau_y\sigma_x + v_{2z}'\tau_z\sigma_x)\mathbf{k}\cdot\mathbf{L}', \tag{21}$$

where $L_i' \equiv |\epsilon_{ijk}|\{L_j, L_k\}$. The linear dispersion of this 12-fold fermion along high-symmetry lines is given in Fig. 5. Compared with Fig. 3b, the two 12-fold fermions have different responses to linear dispersion along the high-symmetry line [111], which result from $N_{\rho_1}(T_{1u}^-) \neq N_{\rho_2}(T_{1u}^-)$ in Eqs. (15) and (20). These qualitative differences distinguish the two 12-fold fermions (14) and (19) coming from two different projective classes of $O_h \times Z_2^T$ with different sets of symmetry invariants.

Actually, if the little co-group is $G_K = O_h \times Z_2^T \times SU(2)$, instead of $O_h \times Z_2^T$, a 12-dimensional irRep may also appear in type-II MSGs without SOC. The 12-fold fermion can be realized at the R point of type II MSGs 222.99, 223.105 (or H point of 230.146)[41]. In fact, there is a
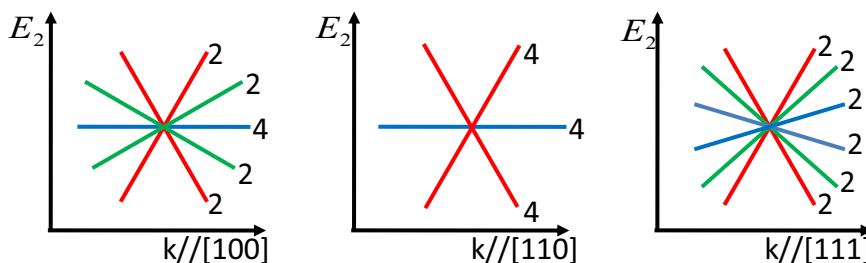

Fig. 5 | 12-fold fermion in spin-space group 229.2.2.36[87]. The schematic dispersion of the 12-fold fermion along three high-symmetry lines [100], [110], [111]. Along [100], the 12-fold fermion splits into one 4-fold band colored in blue, two 2-fold bands colored in red, and two 2-fold bands colored in green. Along [110], the 12-fold fermion splits into one 4-fold band colored in blue and two 4-fold bands colored in red. Along [111], the 12-fold fermion splits into two 2-fold bands colored in red, two 2-fold bands colored in green, and two 2-fold bands colored in blue.

6-dim irRep of $O_h \times Z_2^T$ in the projective class denoted by invariants $\vec{\eta} = (+1, +1, +1, +1, -1)$

$$\rho_3(C_{2i}) = \tau_0 \exp(-iL_i\pi), \rho_3(C_{2\mathbf{n}}) = \tau_z \exp(-i\mathbf{L} \cdot \mathbf{n}\pi),$$
$$\rho_3(I) = \tau_x 1_{3\times3}, \rho_3(T)K = \tau_0 1_{3\times3} K. \quad (22)$$

With spin degrees of freedom, the symmetry group is $O_h \times Z_2^T \times SU(2)$, the band degeneracies at high-symmetry points are 12-fold.

We compare the two 12-fold fermions coming from two different projective classes (14) and (22). Following the general argument, $\rho_1 \otimes \rho_1^*$ and $\rho_3 \otimes \rho_3^*$ are decomposed into linear irReps of $O_h \times Z_2^T$:

$$\rho_1 \otimes \rho_1^* = \cdots \oplus 2T_{2g}^+ \oplus \cdots, \quad (23)$$

$$\rho_3 \otimes \rho_3^* = \cdots \oplus T_{2g}^+ \oplus \cdots. \quad (24)$$

In Eqs. (23), (24), $N_{\rho_1}(T_{2g}^+) \neq N_{\rho_3}(T_{2g}^+)$, so the two quasiparticles have different spectra under an external $\mu = T_{2g}^+$-field (+ means even under time reversal), which can be a strain tensor field ($\epsilon_{yz}, \epsilon_{xz}, \epsilon_{xy}$) with the components $\phi_1^\mu = \epsilon_{yz}, \phi_2^\mu = \epsilon_{xz}, \phi_3^\mu = \epsilon_{xy}$. To be more specific, according to Eq. (13), for projective class ρ_1(14) the coupling takes the form

$$\hat{H}_1 = v_1 \Big(\epsilon_{yz}\tau_0\sigma_0\{L_y, L_z\} + \epsilon_{zx}\tau_0\sigma_0\{L_z, L_x\}$$
$$+ \epsilon_{xy}\tau_0\sigma_0\{L_x, L_y\} \Big) + v_2 \Big(\epsilon_{yz}\tau_x\sigma_0 L_x$$
$$+ \epsilon_{zx}\tau_x\sigma_0 L_y + \epsilon_{xy}\tau_x\sigma_0 L_z \Big), \quad (25)$$

for projective class ρ_3 (22) we have

$$\hat{H}_3 = v_3 \Big(\epsilon_{yz}\tau_0\{L_y, L_z\} + \epsilon_{zx}\tau_0\{L_z, L_x\} + \epsilon_{xy}\tau_0\{L_x, L_y\} \Big). \quad (26)$$

We plot the spectrum of band splitting of $\hat{H}_1$ (colored in red) and $\hat{H}_3$ (colored in blue) under ($\epsilon_{yz}, \epsilon_{xz}, \epsilon_{xy}$) = ($\epsilon, \epsilon, \epsilon$) for $v_1 = v_3 = 1, v_2 = \frac{1}{3}$ and $\epsilon \in [0, \frac{\sqrt{3}}{3}]$. From Fig. 6, we see that the two 12-fold fermions are qualitatively different under an external strain tensor field.
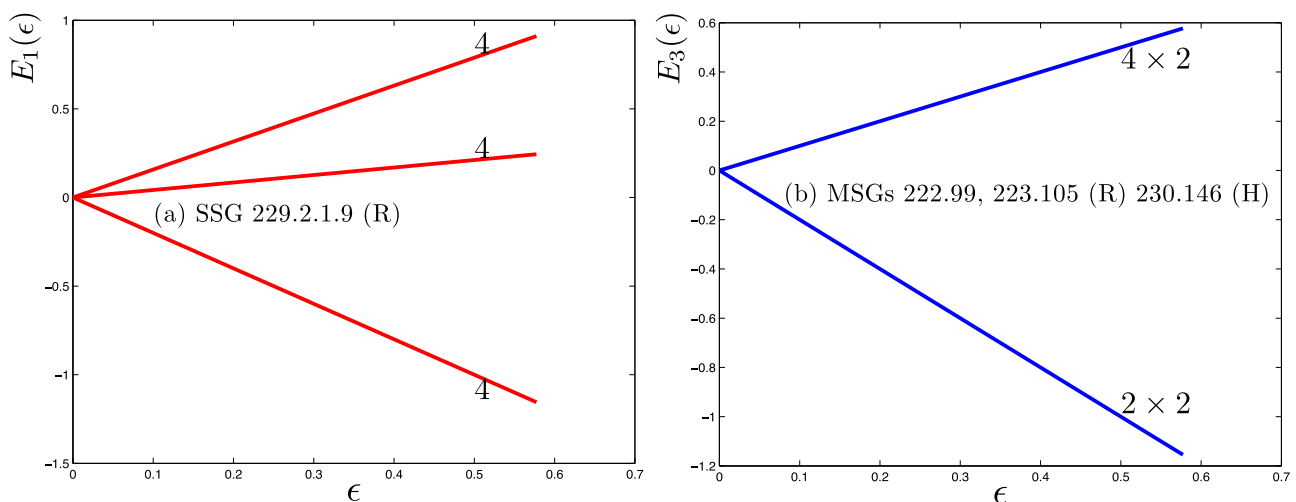
Material candidates

It would be helpful for experimentalists if we could list a few candidate materials where any one of the 218 SSG-only fermions may be discovered. In fact, a comprehensive search is possible using (i) Supplementary Tables III–XXVI of this work, (ii) the database MAGNDATA where over 2000 experimentally discovered magnetic structures are registered, and (iii) the enumeration of all SSGs in ref. 86. First, we sort out all realistic magnetic structures having non-coplanar magnetic structures, which amount to 206 in total. Next, for any one of them, we ask if the hosting SSG is isomorphic to a type-IV MSG. Then, we ask if the point-group part of the SSG is any one of the following: $P \times Z_2^T$ with $P = C_{3h,4h,6h}, D_{3,4,6,3d,3h,4h,6h}, O, O_h$. Finally, we compute the symmetry invariants contributed by the spin operations. If any SSG contains the invariants marked as RED in Supplementary Tables III–XIV, the corresponding material hosts an SSG-only fermion according to our theory. A comprehensive search following the above protocol has been performed, yielding one material: Ce$_3$NIn. The SSG-only co-representation in this material is discussed in Supplementary Note 5. Interestingly, during the revision process of this work, this same material has been proposed as an unconventional p-wave magnet[95]. The scarcity of candidate materials is related to the fact that only a small fraction of magnetic materials have their magnetic structures detected. There are only 2000 materials with known magnetic structures, in contrast to the number of 200000 materials with known crystal structures.

Discussion

We use symmetry invariants to label projective classes of $P \times Z_2^T$ and find 218 new types of quasiparticles only realized in the electronic bands of non-coplanar ($S_0 = \{E\}$) SSGs whose magnetic unit cells are only 2 times the size of the crystal unit cells. The non-coplanar SSGs are isomorphic to type IV MSGs and the little co-groups at high-symmetry points are of the form $G_{\mathbf{K}} = P \times Z_2^T$. For each projective class of $P \times Z_2^T$, the irRep ρ and the Clebsch-Gordon coefficients of the reducible Rep $\rho \otimes \rho^*$ are obtained by the eigenfunction method[7,94].

Our procedure can be extended to study Rep theory of other types of SSGs[86,87], including the non-coplanar SSGs isomorphic to type I or type III MSGs, and the SSGs with nontrivial spin-only groups S_0, namely the collinear and coplanar SSGs. In the following, we comment on these two cases separately.

Fig. 6 | Spectra of two 12-fold fermions under a strain tensor field ($\epsilon_{yz}, \epsilon_{xz}, \epsilon_{xy}$). **a** 12-fold fermion with a symmetry group $O_h \times Z_2^T$ only realizable in SSGs, coming from projective class ρ_1 in Eq. (14). Under coupling (25), the 12-fold fermion splits into three 4-fold bands colored in red. **b** symmetry group is $O_h \times Z_2^T \times SU(2)$, a 6-dimensional irRep (22) of $O_h \times Z_2^T$ splits into 4-fold and 2-fold bands under coupling (26). Due to extra SU(2) spin symmetry, the 12-fold fermion splits into 4×2-fold and 2×2-fold bands colored in blue.

The type I MSGs are 230 SGs, and the little co-groups at high-symmetry points are 32 crystallographic point groups. Since all the projective classes of the 32-point groups have already been realized in the 230 SGs, one cannot obtain any new symmetry invariants (new quasiparticle types).

For the non-coplanar SSGs isomorphic to type III MSGs, the little co-groups $G_\mathbf{K}$ at high-symmetry point $\mathbf{K}$ can be 58 type III magnetic point groups of the form $H + T(P - H)$, where H is a subgroup of the point group P containing half of the elements in P, the other half $P - H$ followed by time reversal T. There are in total 380 projective classes for the 58 type III magnetic point groups. From Eqs. (8), (9), (10), and (11), we calculate lattice-part invariants η^t and spin-part invariants η^s, then obtain the full invariants $\eta = \eta^t \eta^s$. Using the symmetry invariants, we have confirmed that 260 classes are realizable in type III MSGs or at non-time-reversal-invariant high-symmetry points of type II and IV MSGs. There are 120 sets of invariants that cannot be realized in MSGs. In Supplementary Table XXVII, we give definitions of symmetry invariants of 58 type III magnetic point groups. If the symmetry invariants of a group cannot be completely realized in MSGs, the values of symmetry invariants are marked in BLUE if they are realizable via MSGs, and are marked in RED if they are realizable by SSGs only. The BLACK sets of invariants cannot be realized by either MSGs or SSGs. We find an additional 108 classes of new quasiparticles with type III magnetic point group symmetries only realizable in the electronic bands of SSGs. If the minimal dimension of irReps of the same class is FOUR or higher, we provide the degree of degeneracy, the lowest-order dispersion, and the direction of nodal lines. An example is a four-fold degenerate 7-nodal-line-nexus fermion protected by $T_d \times Z_2^{IT}$ (No.57 type III magnetic point group in Supplementary Table XXVII), only realizable in SSGs, with three nodal lines along k_x, k_y, k_z directions and four along $k_x + k_y + k_z$, $k_x + k_y - k_z$, $k_x - k_y + k_z$, and $k_x - k_y - k_z$ directions.

For coplanar SSGs, the spin-only group is $S_0 = Z_2^{C_{2z}T} = \{E, C_{2z}T\}$, and for collinear SSGs, the spin-only group is $S_0 = SO(2) \rtimes Z_2^{C_{2x}T}$ with $Z_2^{C_{2x}T} = \{E, C_{2x}T\}$. The nontrivial S_0 will generally give rise to extra symmetry invariants and may also affect the dimensions of irReps (see Supplementary Note 6.B for more discussions). Due to S_0 and the fact that the magnetic unit cell of a general SSG is enlarged compared to the original crystal unit cell, the little co-group of SSG at a high-symmetry point $\mathbf{K}$ is generally not isomorphic to $P \times Z_2^T$ or type III magnetic point groups. Our approach also applies to these SSGs.

Methods

Projective Reps and 2nd group cohomology

For a projective Rep of a finite group G, an element $g \in G$ is represented by $\rho(g)$ if g is a unitary element and is represented by $\rho(g)K$ if g is anti-unitary, where K is the complex-conjugate operator satisfying $KU = U^*K$ with U an arbitrary matrix and U^* its complex conjugation.

The multiplication of (projective) Reps of g_1 and g_2 depends on if they are unitary or anti-unitary. If we define a unitarity indicator ζ_g

$$\zeta_g = \begin{cases} 0, & \text{if } g \text{ is unitary,} \\ 1, & \text{if } g \text{ is anti-unitary}, \end{cases} \quad (27)$$

and the corresponding operator K^{ζ_g}

$$K^{\zeta_g} = \begin{cases} \text{identity operator}, & \text{if } \zeta_g = 0, \\ K, & \text{if } \zeta_g = 1, \end{cases} \quad (28)$$

then we have the multiplication rule of a projective Rep,

$$\rho(g_1)K^{\zeta_{g_1}}\rho(g_2)K^{\zeta_{g_2}} = \rho(g_1g_2)e^{i\theta_2(g_1,g_2)}K^{\zeta_{g_1g_2}}, \quad (29)$$

where the U(1) phase factor $\omega_2(g_1, g_2) \equiv e^{i\theta_2(g_1, g_2)}$ is a function of two group variables and is called the factor system. If $\omega_2(g_1, g_2) = 1$ for any $g_1, g_2 \in G$, then the above projective Rep becomes a linear Rep.

Substituting the above results into the associativity relation of the sequence of operations $g_1 \times g_2 \times g_3$, we can obtain

$$\begin{aligned} & \rho(g_1)K^{\zeta_{g_1}}\rho(g_2)K^{\zeta_{g_2}}\rho(g_3)K^{\zeta_{g_3}} \\ &= \rho(g_1g_2g_3)\omega_2(g_1, g_2)\omega_2(g_1g_2, g_3)K^{\zeta_{g_1g_2g_3}} \\ &= \rho(g_1g_2g_3)\omega_2(g_1, g_2g_3)\omega_2^{(-1)^{\zeta_{g_1}}}(g_2, g_3)K^{\zeta_{g_1g_2g_3}}, \end{aligned} \quad (30)$$

namely,

$$\omega_2(g_1, g_2)\omega_2(g_1g_2, g_3) = \omega_2^{(-1)^{\zeta_{g_1}}}(g_2, g_3)\omega_2(g_1, g_2g_3). \quad (31)$$

Eq. (31) is the general relation that the factor systems of any finite group (no matter unitary or anti-unitary) should satisfy. The solution of the above equations is called 2-cocyles. If we introduce a gauge transformation $\rho'(g)K^{\zeta_g} = \rho(g)\Omega_1(g)K^{\zeta_g}$, where the phase factor $\Omega_1(g) = e^{i\theta_1(g)}$ depends on a single group variable, then the factor system changes into

$$\omega_2'(g_1, g_2) = \omega_2(g_1, g_2)\Omega_2(g_1, g_2), \quad (32)$$

with

$$\Omega_2(g_1, g_2) = \frac{\Omega_1(g_1)\Omega_1^{(-1)^{\zeta_{g_1}}}(g_2)}{\Omega_1(g_1g_2)}. \quad (33)$$

The quantity $\Omega_2(g_1, g_2)$ defined above are called 2-coboundaries. The equivalent relations (32) and (33) define the equivalent classes of the solutions of (31). The number of equivalent classes for a finite group is usually finite.

Usually, the so-called standard gauge choice is adopted, where $\omega_2(E, g) = \omega_2(g, E) = 1$ for any $g \in G$. This is equivalent to requiring that E is always represented as the identity matrix.

Two 2-cocycles $\omega_2'(g_1, g_2)$ and $\omega_2(g_1, g_2)$ are equivalent if they differ by a 2-coboundary, see Eq. (32). The equivalent classes of the 2-cocycles $\omega_2(g_1, g_2)$ form the second group cohomology $\mathcal{H}^2(G, U(1))$.

Writing $\omega_2(g_1, g_2) = e^{i\theta_2(g_1, g_2)}$, where $\theta_2(g_1, g_2) \in [0, 2\pi)$, then the cocycle Eqs. (31) can be written in terms of linear equations,

$$(-1)^{\zeta_{g_1}}\theta_2(g_2, g_3) - \theta_2(g_1g_2, g_3) + \theta_2(g_1, g_2g_3) - \theta_2(g_1, g_2) = 0. \quad (34)$$

Similarly, if we write $\Omega_1(g_1) = e^{i\theta_1(g_1)}$ and $\Omega_2(g_1, g_2) = e^{i\theta_2(g_1, g_2)}$, then the 2-coboundary (33) can be written as

$$\Theta_2(g_1, g_2) = (-1)^{\zeta_{g_1}}\theta_1(g_2) - \theta_1(g_1g_2) + \theta_1(g_1). \quad (35)$$

The equal sign in Eqs. (34) and (35) means equal mod 2π. From these linear equations, we can obtain the solution space of the cocycle equations, as well as the classes that the solutions belong to. The set of classes forms a finite Abelian group, which labels the classification of the projective Reps (the "projective classes" of G).

Symmetry Invariants

The second group-cohomology group is generated by a set of invariants, dubbed projective symmetry invariants, or symmetry invariants for short. The invariants are special combinations of the cocycles variables $\omega_2(g_1, g_2)$. For any cocycle solutions, the invariants are, by definition, invariant under the gauge transformation (32) and (33), and their values must be equal to roots of 1. Therefore, the values of the invariants are fixed for a given class of factor systems $\omega_2(g_1, g_2)$. On the other hand, the values of the complete set of symmetry invariants uniquely determine the projective class to which a factor system (and the corresponding projective Reps) belongs.

For crystallographic point groups, all the invariants take $\mathbb{Z}_2$ values, namely ± 1. Once the values for the complete set of symmetry

invariants are given, the factor systems in the corresponding projective class can be easily obtained (up to gauge transformations). In the following we give three examples.

(I) The unitary group $D_2 = \{E, C_{2x}\} \times \{E, C_{2y}\}$. For the unitary Abelian group $D_2 = \{E, C_{2x}\} \times \{E, C_{2y}\} = \{E, C_{2x}, C_{2y}, C_{2z}\}$, the classification of 2-cocycles is

$$\mathcal{H}^2(D_2, \mathrm{U}(1)) = \mathbb{Z}_2, \tag{36}$$

where the 2-cocycle equations can be simplified into $\left(\frac{\omega_2(C_{2x}, C_{2y})}{\omega_2(C_{2y}, C_{2x})}\right)^2 = 1$ plus some coboundary relations. Therefore, there is only one independent symmetry invariant, namely,

$$\eta_{C_{2x}, C_{2y}} = \frac{\omega_2(C_{2x}, C_{2y})}{\omega_2(C_{2y}, C_{2x})} = \pm 1. \tag{37}$$

The projective class with invariant $\eta_{C_{2x}, C_{2y}} = -1$ is nontrivial, which indicates that the projective Rep matrices of C_{2x} and C_{2y} are anti-commuting, $\rho(C_{2x})\rho(C_{2y}) = -\rho(C_{2y})\rho(C_{2x})$ although C_{2x} and C_{2y} are commuting as group elements of D_2. As an example, the factor system in this class can be chosen as: $\omega_2(C_{2y}, C_{2x}) = \omega_2(C_{2y}, C_{2z}) = \omega_2(C_{2z}, C_{2x}) = \omega_2(C_{2z}, C_{2z}) = -1$, and all the other components are equal to 1. The projective irReps belonging to this class are 2-dimensional.

On the other hand, the projective class with invariant $\eta_{C_{2x}, C_{2y}} = 1$ is trivial. A typical factor system in this class is the one with all components equal to 1. In the trivial class, all the irReps, including the linear Reps as a special case, are 1-dimensional.

It should be mentioned that the choices of symmetry invariants may not be unique. For the D_2 group, since the relation $\eta_{C_{2x}, C_{2y}} = \eta_{C_{2x}, C_{2z}} = \eta_{C_{2y}, C_{2z}}$ is always valid, any one of $\eta_{C_{2x}, C_{2y}}, \eta_{C_{2x}, C_{2z}}, \eta_{C_{2y}, C_{2z}}$ can be chosen as the symmetry invariant.

(II) The anti-unitary group $Z_2^T = \{E, T\}$. The simplest anti-unitary group is the time-reversal group $Z_2^T = \{E, T\}$, the classification of its 2-cocycles is

$$\mathcal{H}^2(Z_2^T, \mathrm{U}(1)) = \mathbb{Z}_2, \tag{38}$$

where the 2-cocycle equations can be simplified into $\left(\omega_2(T, T)\right)^2 = 1$ under the standard gauge. Therefore, the symmetry invariant is given by

$$\eta_T = \omega_2(T, T) = \pm 1. \tag{39}$$

Here projective class with $\eta_T = -1$ stands for the Kramers class which guarantees the double-degeneracy, while projective class with $\eta_T = 1$ stands for the trivial class where no degeneracy is guaranteed.

(III) The anti-unitary group $D_2 \times Z_2^T$. Now we consider the group $D_2 \times Z_2^T$, the classification of 2-cocycles is

$$\mathcal{H}^2(D_2 \times Z_2^T, \mathrm{U}(1)) = \mathbb{Z}_2^4. \tag{40}$$

Under the standard gauge, the 2-cocycle equations can be simplified into

$$\left(\frac{\omega_2(C_{2x}, C_{2y})}{\omega_2(C_{2y}, C_{2x})}\right)^2 = 1, (\omega_2(T, T))^2 = 1, (\omega_2(TC_{2x}, TC_{2x}))^2 = 1, (\omega_2(TC_{2y}, TC_{2y}))^2 = 1$$

plus some coboundary relations. Therefore, the resultant symmetry invariants are

$$\begin{aligned} \eta_{C_{2x}, C_{2y}} &= \frac{\omega_2(C_{2x}, C_{2y})}{\omega_2(C_{2y}, C_{2x})} = \pm 1, \\ \eta_T &= \omega_2(T, T) = \pm 1, \\ \eta_{TC_{2x}} &= \omega_2(TC_{2x}, TC_{2x}) = \pm 1, \\ \eta_{TC_{2y}} &= \omega_2(TC_{2y}, TC_{2y}) = \pm 1. \end{aligned} \tag{41}$$

There are totally 16 projective classes, 15 of them are nontrivial and the rest one, the trivial class with all the invariants equal to 1, is gauge equivalent to linear Reps.

Data availability
All results shown in this work are mathematical in nature, and no external data has been used to generate them.

Code availability
The code used to calculate is available from the authors upon reasonable request.

References

1. Sakurai, J. J. & Napolitano, J. *Modern Quantum Mechanics* (Addison-Wesley, 2011).
2. Weinberg, S. *The Quantum theory of fields. Vol. 1: Foundations.* (Cambridge University Press, 2005).
3. Castro Neto, A. H., Guinea, F., Peres, N. M. R., Novoselov, K. S. & Geim, A. K. The electronic properties of graphene. *Rev. Mod. Phys.* **81**, 109–162 (2009).
4. Huang, Shin-Ming et al. A weyl fermion semimetal with surface fermi arcs in the transition metal monopnictide taas class. *Nat. Commun.* **6**, 7373 (2015).
5. Chen, X., Gu, Zheng-Cheng & Wen, Xiao-Gang Classification of gapped symmetric phases in one-dimensional spin systems. *Phys. Rev. B* **83**, 035107 (2011).
6. Chen, X., Gu, Zheng-Cheng, Liu, Zheng-Xin & Wen, Xiao-Gang Symmetry protected topological orders and the group cohomology of their symmetry group. *Phys. Rev. B* **87**, 155114 (2013).
7. Yang, J. & Liu, Zheng-Xin Irreducible projective representations and their physical applications. *J. Phys. A Math. Theor.* **51**, 025207 (2018).
8. Yang, J., Liu, Z.-X. & Fang, C. Unlocking of time reversal, space-time inversion and rotation invariants in magnetic materials. Preprint at https://arxiv.org/abs/2009.07864 (2020).
9. Yang, J., Fang, C. & Liu, Zheng-Xin Symmetry-protected nodal points and nodal lines in magnetic materials. *Phys. Rev. B* **103**, 245141 (2021).
10. Ouyang, Y., Wang, Qing-Rui, Gu, Zheng-Cheng & Qi, Y. Computing classification of interacting fermionic symmetry-protected topological phases using topological invariants. *Chin. Phys. Lett.* **38**, 127101 (2021).
11. Chen, Z. Y., Zhang, Z., Yang, S. A. & Zhao, Y. X. Classification of time-reversal-invariant crystals with gauge structures. *Nat. Commun.* **14**, 743 (2023).
12. Slager, Robert-Jan, Mesaros, A., Juričić, V. & Zaanen, J. The space group classification of topological band-insulators. *Nat. Phys.* **9**, 98–102 (2013).
13. Young, S. M. et al. Dirac semimetal in three dimensions. *Phys. Rev. Lett.* **108**, 140405 (2012).
14. Yang, Bohm-Jung & Nagaosa, N. Classification of stable three-dimensional dirac semimetals with nontrivial topology. *Nat. Commun.* **5**, 4898 (2014).
15. Fang, C., Chen, Y., Kee, Hae-Young & Fu, L. Topological nodal line semimetals with and without spin-orbit coupling. *Phys. Rev. B* **92**, 081201 (2015).
16. Watanabe, H., Po, HoiChun, Zaletel, M. P. & Vishwanath, A. Filling-enforced gaplessness in band structures of the 230 space groups. *Phys. Rev. Lett.* **117**, 096404 (2016).
17. Bradlyn, B. et al. Beyond dirac and weyl fermions: Unconventional quasiparticles in conventional crystals. *Science* **353**, aaf5037 (2016).
18. Kruthoff, J., de Boer, J., van Wezel, J., Kane, C. L. & Slager, Robert-Jan Topological classification of crystalline insulators through band structure combinatorics. *Phys. Rev. X* **7**, 041069 (2017).

19. Bradlyn, B. et al. Topological quantum chemistry. *Nature* **547**, 298–305 (2017).

20. Armitage, N. P., Mele, E. J. & Vishwanath, A. Weyl and dirac semimetals in three-dimensional solids. *Rev. Mod. Phys.* **90**, 015001 (2018).

21. Song, Z., Zhang, T. & Fang, C. Diagnosis for nonmagnetic topological semimetals in the absence of spin-orbital coupling. *Phys. Rev. X* **8**, 031069 (2018).

22. Zhang, T. et al. Catalogue of topological electronic materials. *Nature* **566**, 475–479 (2019).

23. Vergniory, M. G. et al. A complete catalogue of high-quality topological materials. *Nature* **566**, 480–485 (2019).

24. Tang, F., Po, HoiChun, Vishwanath, A. & Wan, X. Comprehensive search for topological materials using symmetry indicators. *Nature* **566**, 486–489 (2019).

25. Cano, J. & Bradlyn, B. Band representations and topological quantum chemistry. *Annu. Rev. Condens. Matter Phys.* **12**, 225–246 (2021).

26. Fan, D., Wan, X. & Tang, F. Catalog of maximally charged weyl points hosting nearly emanating nodal lines in phonon spectra. *Phys. Rev. B* **108**, 104110 (2023).

27. Tang, P., Zhou, Q., Xu, G. & Zhang, Shou-Cheng Dirac fermions in an antiferromagnetic semimetal. *Nat. Phys.* **12**, 1100–1104 (2016).

28. Liang, L. & Yu, Y. Semimetal with both rarita-schwinger-weyl and weyl excitations. *Phys. Rev. B* **93**, 045113 (2016).

29. Watanabe, H., Po, HoiChun & Vishwanath, A. Structure and topology of band structures in the 1651 magnetic space groups. *Sci. Adv.* **4**, eaat8685 (2018).

30. Hua, G. et al. Dirac semimetal in type-iv magnetic space groups. *Phys. Rev. B* **98**, 201116 (2018).

31. Geilhufe, R. M., Guinea, F. & Juričić, V. Hund nodal line semimetals: The case of a twisted magnetic phase in the double-exchange model. *Phys. Rev. B* **99**, 020404 (2019).

32. Cano, J., Bradlyn, B. & Vergniory, M. G. Multifold nodal points in magnetic materials. *APL Mater.* **7**, 101125 (2019).

33. Xu, Y. et al. High-throughput calculations of magnetic topological materials. *Nature* **586**, 702–707 (2020).

34. Bouhon, A., Lange, G. F. & Slager, Robert-Jan Topological correspondence between magnetic space group representations and subdimensions. *Phys. Rev. B* **103**, 245127 (2021).

35. Tang, F. & Wan, X. Exhaustive construction of effective models in 1651 magnetic space groups. *Phys. Rev. B* **104**, 085137 (2021).

36. Jiang, Y., Fang, Z. & Fang, C. A $\mathbf{k} \cdot \mathbf{p}$ effective hamiltonian generator. *Chin. Phys. Lett.* **38**, 077104 (2021).

37. Elcoro, L. et al. Magnetic topological quantum chemistry. *Nat. Commun.* **12**, 5965 (2021).

38. Liu, Gui-Bin, Zhang, Z., Yu, Zhi-Ming, Yang, S. A. & Yao, Y. Systematic investigation of emergent particles in type-iii magnetic space groups. *Phys. Rev. B* **105**, 085117 (2022).

39. Zhang, Z., Liu, Gui-Bin, Yu, Zhi-Ming, Yang, S. A. & Yao, Y. Encyclopedia of emergent particles in type-iv magnetic space groups. *Phys. Rev. B* **105**, 104426 (2022).

40. Lenggenhager, P. M., Liu, X., Neupert, T. & Bzdušek, Tomáš. Triple nodal points characterized by their nodal-line structure in all magnetic space groups. *Phys. Rev. B* **106**, 085128 (2022).

41. Tang, F. & Wan, X. Complete classification of band nodal structures and massless excitations. *Phys. Rev. B* **105**, 155156 (2022).

42. Bernevig, B. A., Felser, C. & Beidenkopf, H. Progress and prospects in magnetic topological materials. *Nature* **603**, 41–51 (2022).

43. Fan, D., Wan, X. & Tang, F. All hourglass bosonic excitations in the 1651 magnetic space groups and 528 magnetic layer groups. *Phys. Rev. Mater.* **6**, 124201 (2022).

44. Lin, Kuan-Sen et al. Spin-resolved topology and partial axion angles in three-dimensional insulators. *Nat. Commun.* **15**, 550 (2024).

45. BRADLEY, C. J. & DAVIES, B. L. Magnetic groups and their corepresentations. *Rev. Mod. Phys.* **40**, 359–379 (1968).

46. Lifshitz, R. "Magnetic point groups and space groups" in Encyclopedia of Condensed Matter Physics (Elsevier, 2024).

47. Bradley, C. & Cracknell, A. *The Mathematical Theory of Symmetry in Solids: Representation Theory for Point Groups and Space Groups*, EBSCO ebook academic collection (OUP Oxford, 2010).

48. Litvin, D.B. *Magnetic Group Tables. 1-, 2-and 3-Dimensional Magnetic Subperiodic Groups and Magnetic Space Groups* (International Union of Crystallography, Chester, 2013).

49. Gallego, S. V. et al. Magndata: towards a database of magnetic structures. i. the commensurate case. *J. Appl. Crystallogr.* **49**, 1750–1776 (2016).

50. González-Platas, J., Katcho, N. A. & Rodríguez-Carvajal, J. Extension of hall symbols of crystallographic space groups to magnetic space groups. *J. Appl. Crystallogr.* **54**, 338–342 (2021).

51. Liu, Gui-Bin, Zhang, Z., Yu, Zhi-Ming & Yao, Y. MSGCorep: A package for corepresentations of magnetic space groups. *Comput. Phys. Commun.* **288**, 108722 (2023).

52. Liu, P., Li, J., Han, J., Wan, X. & Liu, Q. Spin-group symmetry in magnetic materials with negligible spin-orbit coupling. *Phys. Rev. X* **12**, 021016 (2022).

53. Liu, P., Zhang, A., Han, J. & Liu, Q. Chiral dirac-like fermion in spin-orbit-free antiferromagnetic semimetals. *Innovation* **3**, 100343 (2022).

54. Corticelli, A., Moessner, R. & McClarty, P. A. Spin-space groups and magnon band topology. *Phys. Rev. B* **105**, 064430 (2022).

55. Šmejkal, L., Sinova, J. & Jungwirth, T. Beyond conventional ferromagnetism and antiferromagnetism: A phase with nonrelativistic spin and crystal rotation symmetry. *Phys. Rev. X* **12**, 031042 (2022).

56. Hayami, S., Yanagi, Y. & Kusunose, H. Momentum-dependent spin splitting by collinear antiferromagnetic ordering. *J. Phys. Soc. Jpn.* **88**, 123702 (2019).

57. Hayami, S., Yanagi, Y. & Kusunose, H. Bottom-up design of spin-split and reshaped electronic band structures in antiferromagnets without spin-orbit coupling: Procedure on the basis of augmented multipoles. *Phys. Rev. B* **102**, 144441 (2020).

58. Šmejkal, L., González-Hernández, R., Jungwirth, Tomás. & Sinova, J. Crystal time-reversal symmetry breaking and spontaneous hall effect in collinear antiferromagnets. *Sci. Adv.* **6**, eaaz8809 (2020).

59. Mazin, I. I., Koepernik, K., Johannes, M. D., González-Hernández, R. & Šmejkal, L. Prediction of unconventional magnetism in doped FeSb$_2$. *Proc. Natl. Acad. Sci. USA* **118**, e2108924118 (2021).

60. Šmejkal, L., Sinova, J. & Jungwirth, T. Emerging research landscape of altermagnetism. *Phys. Rev. X* **12**, 040501 (2022).

61. Mazin, I. (The PRX Editors), Editorial: Altermagnetism—a new punch line of fundamental magnetism. *Phys. Rev. X* **12**, 040002 (2022).

62. Hariki, A. et al. X-ray magnetic circular dichroism in altermagnetic α-mnte. *Phys. Rev. Lett.* **132**, 176701 (2024).

63. Papaj, Michał. Andreev reflection at the altermagnet-superconductor interface. *Phys. Rev. B* **108**, L060508 (2023).

64. Ghorashi, SayedAliAkbar, Hughes, T. L. & Cano, J. Altermagnetic routes to majorana modes in zero net magnetization. *Phys. Rev. Lett.* **133**, 106601 (2024).

65. Steward, CharlesR. W., Fernandes, R. M. & Schmalian, J. örg Dynamic paramagnon-polarons in altermagnets. *Phys. Rev. B* **108**, 144418 (2023).

66. Fernandes, R. M., de Carvalho, V. S., Birol, T. & Pereira, R. G. Topological transition from nodal to nodeless zeeman splitting in altermagnets. *Phys. Rev. B* **109**, 024404 (2024).

67. Fang, Y., Cano, J. & Ghorashi, SayedAliAkbar Quantum geometry induced nonlinear transport in altermagnets. *Phys. Rev. Lett.* **133**, 106701 (2024).

68. Reichlová, H. et al. Macroscopic time reversal symmetry breaking by staggered spin-momentum interaction. Preprint at https://arxiv.org/abs/2012.15651v2 (2020).

69. Feng, Z. et al. An anomalous hall effect in altermagnetic ruthenium dioxide. *Nat. Electron.* **5**, 735–743 (2022).

70. Betancourt, R. D. Gonzalez et al. Spontaneous anomalous hall effect arising from an unconventional compensated magnetic phase in a semiconductor. *Phys. Rev. Lett.* **130**, 036702 (2023).

71. Zhu, Yu-Peng et al. Observation of plaid-like spin splitting in a noncoplanar antiferromagnet. *Nature* **626**, 523–528 (2024).

72. Zhang, A. et al. Chiral dirac fermion in a collinear antiferromagnet. *Chin. Phys. Lett.* **40**, 126101 (2023).

73. Guo, Peng-Jie, Wei, Yi-Wen, Liu, K., Liu, Zheng-Xin & Lu, Zhong-Yi Eightfold degenerate fermions in two dimensions. *Phys. Rev. Lett.* **127**, 176401 (2021).

74. Guo, Peng-Jie, Liu, Zheng-Xin & Lu, Zhong-Yi Quantum anomalous hall effect in collinear antiferromagnetism. *Npj Comput. Mater.* **9**, 70 (2023).

75. Xiao, Z., Zhao, J., Li, Y., Shindou, R. & Song, Zhi-Da Spin space groups: Full classification and applications. *Phys. Rev. X* **14**, 031037 (2024).

76. Chen, X. et al. Enumeration and representation theory of spin space groups. *Phys. Rev. X* **14**, 031038 (2024).

77. Chen, X., Ren, J., Li, J., Liu, Y. & Liu, Q. Spin space group theory and unconventional magnons in collinear magnets. Preprint at https://arxiv.org/abs/2307.12366 (2023b).

78. Birman, J.L. *Theory of Crystal Space Groups and Lattice Dynamics: Infra-Red and Raman Optical Processes of Insulating Crystals*, Handbuch der Physik (Springer Berlin Heidelberg, 1984).

79. Hamermesh, M. *Group Theory and Its Application to Physical Problems*, Addison Wesley Series in Physics (Dover Publications, 1989).

80. Zhang, T. et al. Double-weyl phonons in transition-metal monosilicides. *Phys. Rev. Lett.* **120**, 016401 (2018).

81. Rao, Z. et al. Observation of unconventional chiral fermions with long fermi arcs in CoSi. *Nature* **567**, 496–499 (2019).

82. Schröter, NielsB. M. et al. Chiral topological semimetal with multifold band crossings and long fermi arcs. *Nat. Phys.* **15**, 759–765 (2019).

83. Sanchez, D. S. et al. Topological chiral crystals with helicoid-arc quantum states. *Nature* **567**, 500–505 (2019).

84. Brinkman, W. F. & Elliott, R. J. Theory of spin-space groups. *Proc. R. Soc. Lond. Ser. A Math. Phys. Sci.* **294**, 343–358 (1966).

85. Litvin, D. B. & Opechowski, W. Spin groups. *Physica* **76**, 538–554 (1974).

86. Jiang, Y. et al. Enumeration of spin-space groups: Toward a complete description of symmetries of magnetic orders. *Phys. Rev. X* **14**, 031039 (2024).

87. Jiang, Yi. et al. The spin-space group database, https://cmpdc.iphy.ac.cn/ssg (2024).

88. Watanabe, H., Shinohara, K., Nomoto, T., Togo, A. & Arita, R. Symmetry analysis with spin crystallographic groups: Disentangling effects free of spin-orbit coupling in emergent electromagnetism. *Phys. Rev. B* **109**, 094438 (2024).

89. Shinohara, K. et al. Algorithm for spin symmetry operation search. *Acta Crystallogr. Section A Found. Adv.* **80**, 94–103 (2024).

90. Litvin, D. B. Spin point groups. *Acta Crystallogr. Sect. A* **33**, 279–287 (1977).

91. Schiff, H., Corticelli, A., Guerreiro, A., Romhányi, J. & McClarty, P. The spin point groups and their representations. Preprint at https://arxiv.org/abs/2307.12784 (2023).

92. Chen, Jin-Quan, Gao, Mei-Juan & Ma, Guang-Qun The representation group and its application to space groups. *Rev. Mod. Phys.* **57**, 211–278 (1985).

93. Chen, J.Q., Ping, J. & Wang, F. *Group Representation Theory for Physicists* (World Scientific, 2002).

94. Yang, Zhen-Yuan., Yang, J., Fang, C. & Liu, Zheng-Xin. A hamiltonian approach for obtaining irreducible projective representations and the **k·p** perturbation for anti-unitary symmetry groups. *J. Phys. A Math.* **54**, 265202 (2021).

95. Hellenes, A. B., Jungwirth, T., Sinova, J. & Šmejkal, L. P-wave magnets. Preprint at https://arxiv.org/abs/2309.01607 (2024).

Acknowledgements

Author contributions

Z.X.L. and C.F. initiated this work. J.Y. did the major derivation and numerical calculation. All authors discussed the results and participated in the writing of the manuscript.

Competing interests

The authors declare no competing interests.

Additional information

Supplementary information The online version contains supplementary material available at https://doi.org/10.1038/s41467-024-53862-6.

Correspondence and requests for materials should be addressed to Zheng-Xin Liu or Chen Fang.

Peer review information *Nature Communications* thanks the anonymous reviewers for their contribution to the peer review of this work. A peer review file is available.

Reprints and permissions information is available at http://www.nature.com/reprints

Publisher's note Springer Nature remains neutral with regard to jurisdictional claims in published maps and institutional affiliations.